

THE MASS DISTRIBUTION AND ASSEMBLY OF THE MILKY WAY FROM THE PROPERTIES OF THE MAGELLANIC CLOUDS

MICHAEL T. BUSH^{1,2}, PHILIP J. MARSHALL^{1,3}, RISA H. WECHSLER^{1,4}, ANATOLY KLYPIN⁵, AND JOEL PRIMACK⁶

Draft version November 17, 2018

ABSTRACT

We present a new measurement of the mass of the Milky Way (MW) based on observed properties of its largest satellite galaxies, the Magellanic Clouds (MCs), and an assumed prior of a Λ CDM universe. A large, high resolution cosmological simulation of this universe provides a means to statistically sample the dynamical properties of bright satellite galaxies in a large population of dark matter halos. The observed properties of the MCs, including their circular velocity, distance from the center of the MW, and velocity within the MW halo, are used to evaluate the likelihood that a given halo would have each or all of these properties; the posterior PDF for any property of the MW system can thus be constructed. This method provides a constraint on the MW virial mass, $1.2^{+0.7}_{-0.4} \times 10^{12} M_{\odot}$ (68% confidence), which is consistent with recent determinations that involve very different assumptions. In addition, we calculate the posterior PDF for the density profile of the MW and its satellite accretion history. Although typical satellites of $10^{12} M_{\odot}$ halos are accreted over a wide range of epochs over the last 10 Gyr, we find a $\sim 72\%$ probability that the Magellanic Clouds were accreted within the last Gyr, and a 50% probability that they were accreted together.

Subject headings: Galaxy: formation, fundamental parameters, halo — galaxies: dwarf, Magellanic Clouds, evolution — dark matter

1. INTRODUCTION

The contents of the Milky Way (MW) Galaxy and the satellites that fall under its dynamical spell provide a unique testbed for theories of galaxy formation and cosmology. Detailed observations of resolved stars, including proper motions, allow the mass distribution of the galaxy to be measured with ever higher precision (e.g. Kallivayalil et al. 2006; Piatek et al. 2008). Satellite galaxies within the MW have been detected with luminosities three orders of magnitude smaller than in external galaxies (e.g. Belokurov et al. 2007). In addition, determining the detailed phase space distribution of the MW galaxy is critical for interpreting the results of experiments to directly or indirectly detect particle dark matter (e.g. Strigari & Trotta 2009; Vogelsberger et al. 2009; Lisanti et al. 2010; Kuhlen et al. 2010). A full understanding of the MW’s place in the Universe requires not only detailed knowledge of its mass distribution and formation history, but also a sense of how this one well-studied system fits into the full cosmological context.

A variety of methods have been used to put limits on the MW mass, ranging from stellar dynamics and dynamics of satellites (Klypin et al. 2002; Battaglia et al. 2005; Dehnen et al. 2006; Smith et al. 2007; Xue et al. 2008; Watkins et al. 2010; Gnedin et al. 2010) to the dynamics of the local group (Li & White 2008). For example,

Battaglia et al. (2005) and Xue et al. (2008) performed a Jeans analysis of measurements of the radial velocity dispersion profile from satellite galaxies, globular clusters, and blue horizontal branch halo stars to estimate the MW radial density profile. Smith et al. (2007) used measurements of high-velocity halo stars to estimate the MW escape speed assuming an NFW profile. Li & White (2008) took a complementary approach, using the relative position and velocity of the MW and M31, along with the age of the universe, to infer properties of the orbits of the MW-M31 system, which provides constraints on the total mass.

Similarly, there have been a range of studies on the dynamical state of the Magellanic Clouds (MCs). Until recently, the standard picture was that the MCs were objects that have been orbiting the MW for some time (Murai & Fujimoto 1980; Gardiner et al. 1994). This picture was motivated in part by the presence of the Magellanic Stream, a filament of gas extending 150° across the sky. Because it is clearly spatially and chemically associated with the Magellanic Clouds, it has often been interpreted as a tidal tail and taken as an indication that the satellites have been around for several Gyr (see, i.e., Connors et al. 2006). This picture has recently come under fire, largely as a result of detailed measurements of the three-dimensional velocity of the MCs: they are observed to have high velocities not aligned with the Magellanic Stream, indicating that they are not in virial equilibrium (and suggesting alternative formation methods for the Magellanic Stream; see Besla et al. 2007, 2010). Similarly, there is a growing consensus that the MCs accreted as a group: evidence for this comes from both their proximity in phase space (Kallivayalil et al. 2006a), and the result that simulated subhalos in general tend to accrete in groups (D’Onghia & Lake 2008).

In this work, we take a new approach to measure the mass and assembly of the MW. N-body simulations of dark matter structures in a Λ CDM universe have been very successful at reproducing the observed clustering of galaxies (e.g. Kravtsov et al. 2004; Conroy et al. 2006). In two com-

¹ Kavli Institute for Particle Astrophysics and Cosmology, Physics Department, Stanford University, Stanford, CA, 94305, USA
mbusha@stanford.edu, pjms@slac.stanford.edu, rwechsler@stanford.edu

² Institute for Theoretical Physics, University of Zurich, 8057 Zurich, Switzerland

³ Department of Physics, Oxford University, Oxford, OX1 3RH, UK.

⁴ Particle and Particle Astrophysics Department, SLAC National Accelerator Laboratory, Menlo Park, CA, 94025, USA

⁵ Astronomy Department, New Mexico State University, Las Cruces, NM, 88003

⁶ Department of Physics, University of California, Santa Cruz, CA 95064, USA

panion papers, we show that the full probability distribution (PDF) for the number of bright satellites around MW-luminosity hosts predicted by high resolution numerical simulations (Busha et al. 2010) is in excellent agreement with measurements from the SDSS (Liu et al. 2010). This provides evidence that such cosmological simulations realistically represent galaxy halos and their satellites, and that they sample the underlying probability distribution for the properties of halos and subhalos in our Universe. These simulated halo catalogs therefore constitute a *highly informative prior PDF for the parameters of any particular galaxy system*. In this work we show that combining this prior with basic data about the two most massive MW satellites — their masses, velocities, and positions — provides interesting constraints on the MW mass, the distribution of mass within the MW system, and the system’s assembly history. Although we find that the simulation used here provides only a relatively sparse sampling of the underlying PDF, this is the first time that the statistics to study the MW system in this way have been available at all. As high-resolution cosmological simulations probe ever larger volumes, this approach will have increasing power and applicability.

2. SIMULATIONS

Statistical inference from halo dynamical histories requires a large, unbiased, sample of dark matter halos which samples the full range of cosmologically appropriate formation scenarios. Here, we use halos from the Bolshoi simulation (Klypin et al. 2010), which modeled a $250 h^{-1}\text{Mpc}$ comoving box with $\Omega_m = 0.27$, $\Omega_\Lambda = 0.73$, $\sigma_8 = 0.82$, $n = 0.95$, and $h = 0.7$. The simulation volume contained 2048^3 particles, each with mass $1.15 \times 10^8 h^{-1} M_\odot$, and was run using the ART code (Kravtsov et al. 1997). Halos and subhalos were identified using the BDM algorithm (Klypin & Holtzman 1997); see Klypin et al. (2010) for details. One unique aspect of this simulation is the high spatial resolution, which is resolved down to a physical scale of $1 h^{-1}\text{kpc}$. This improves the tracking of halos as they merge with and are disrupted by larger objects, allowing them to be followed even as they pass near the core of the halo. The resulting halo catalog is complete for objects down to a circular velocity of $v_{\text{max}} = 50 \text{ km s}^{-1}$. The large volume probed results in a sample of 2.1 million simulated galaxy halos at the present epoch, including more than 100,000 halos massive enough to host at least one resolved subhalo. We can increase this number further by considering halos identified at different epochs to be independent objects representative of local systems: we use halos from 60 simulation snapshots out to redshift 0.25. Throughout, we define “hosts” as halos that are not within the virial radius of a larger halo, and “satellites” as any object within 300 kpc of a host. This value is chosen to be roughly half the distance between the MW and M31.

3. OBSERVATIONS

We now consider the massive subhalo population of the MW that is modeled by the Bolshoi simulation: objects with $v_{\text{max}} > 50 \text{ km s}^{-1}$. The two brightest MW satellite galaxies, the LMC and SMC, have both been measured to have maximum circular velocities $v_{\text{max}} \gtrsim 60 \text{ km s}^{-1}$ with magnitudes $M_V = -18.5$ and -17.1 , respectively (van der Marel et al. 2002; Stanimirović et al. 2004; van den Bergh 2000). The next brightest satellite is Sagittarius, some 4 magnitudes dimmer, with $v_{\text{max}} \sim 20 \text{ km s}^{-1}$ (Strigari et al. 2007). Similar constraints, albeit with larger error bars, can be made for the

TABLE 1
OBSERVED PROPERTIES OF THE LMC AND SMC.

	LMC	SMC	Reference
v_{max} [km/s]	65 ± 15	60 ± 15	vdM02, S04, HZ06
r_0 [kpc]	50 ± 2	60 ± 2	vdM02
v_r [km/s]*	89 ± 8	23 ± 14	K06a
s [km/s]*	378 ± 36	301 ± 104	K06b

NOTE. — vdM02 = van der Marel et al. (2002); S04 = Stanimirović et al. (2004); K06a,b = Kallivayalil et al. (2006a,2006c) HZ06 = Harris & Zaritsky (2006).

* Errors on v_r , and s have been increased relative to the published values (see text)

other bright classical satellites. The census of nearby objects brighter than $M_V \approx -8$ should be complete well beyond the MW virial radius (Walsh et al. 2009; Tollerud et al. 2008). It is therefore a robust statement that the MW has exactly two satellites with $v_{\text{max}} > 50 \text{ km s}^{-1}$.

Applying this selection criterion to the Bolshoi catalog, we find 36,000 simulated halos that have exactly two satellites with $v_{\text{max}} > 50 \text{ km s}^{-1}$. These $N_{\text{subs}} = 2$ systems represent a first attempt at finding simulated halos that are analogs of the MW in terms of massive satellite content. What other properties of the LMC and SMC might provide information on the mass and assembly history of the MW system? Repeated observations over many years with *HST* and ground-based spectroscopy have given us excellent limits on both the 3D position and velocity of both objects. Indeed, both of these properties are significantly better constrained than are the circular velocities of these objects. We select simulated objects to be MC analogs based on v_{max} , the maximum circular velocity of the object, r_0 , the distance of the object to the center of the MW, v_r , the radial velocity relative to the center of the MW, and s , the total speed of the object. These are summarized in Table 1. In order to be conservative with the uncertainties to account for systematics, we multiply the published formal errors in the radial velocity and speed errors by a factor of two when looking for MC analogs in Bolshoi (included in the errors shown in Table 1). This increase is necessary to bring the velocity measurements of the SMC by Kallivayalil et al. (2006b) and Piatek et al. (2008) into agreement.

4. INFERENCE

As outlined, the Bolshoi halo catalog can be thought of as a set of sample halos drawn from an underlying probability distribution. Each halo is characterized by a set of m parameters \mathbf{x} , which includes the total mass of the halo and the properties of its subhalos, such as their masses, positions, and velocities. We would like to know the posterior PDF for these parameters in one particular system, the Milky Way, for which we have some data \mathbf{d} :

$$\Pr(\mathbf{x}|\mathbf{d}) \propto \Pr(\mathbf{d}|\mathbf{x})\Pr(\mathbf{x}) \quad (1)$$

Since we have $\Pr(\mathbf{x})$ (very conveniently) in the form of a set of n samples drawn from it, we can compute any desired integral over the posterior PDF by assigning each prior sample parameter vector \mathbf{x}_j a weight, or importance, equal to the likelihood $\Pr(\mathbf{d}|\mathbf{x}_j)$ (see e.g. Lewis & Bridle 2002; Suyu et al. 2010):

$$\int f(\mathbf{x})\Pr(\mathbf{x}|\mathbf{d})d^m\mathbf{x} \simeq \frac{\sum_j^n f(\mathbf{x}_j)\Pr(\mathbf{d}|\mathbf{x}_j)}{\sum_j^n \Pr(\mathbf{d}|\mathbf{x}_j)} \quad (2)$$

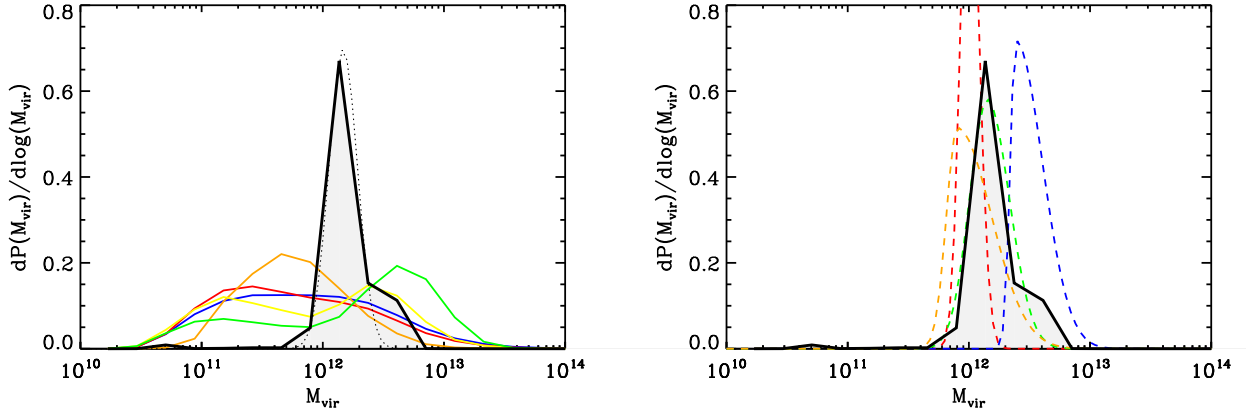


FIG. 1.— *Left:* The MW mass inferred from the properties of its two most luminous satellites, the Magellanic Clouds. Lines show posterior PDFs (weighted histograms of Bolshoi halos) given information about (a) the existence of exactly two satellites with $v_{\max} > 50 \text{ km s}^{-1}$ (blue), (b) the maximum circular velocities v_{\max} of the two satellites (red), (c) the distance of each satellite from the center of the MW (orange), (d) the radial velocity of each satellite (yellow), (e) the speed of each satellite (green), and (f) all of these properties simultaneously (black). The combined properties define a sample of “satellite analogs” and give $M_{\text{MW}} = 1.2^{+0.7}_{-0.4} \times 10^{12} M_{\odot}$ (68% confidence). The dashed line shows a lognormal fit to this distribution, with parameters $\log_{10} M_{\text{MW}} = 12.2 \pm 0.1$. *Right:* Comparison with various estimates for the mass of the MW from the literature. Dashed lines show results from: (a) the radial velocity dispersion profile (Battaglia et al. 2005) (orange); (b) the escape velocity from halo stars (Smith et al. 2007) (red); (c) SDSS blue horizontal branch stars (Xue et al. 2008) (green), and (d) the timing argument (Li & White 2008) (blue). We assume lognormal error distributions, with asymmetric errors given by the quoted upper and lower confidence limits. The solid (black) line shows the posterior PDF for the MW mass from our satellite analogs.

where $f(\mathbf{x})$ is some function of interest. For example, we can represent $\Pr(\mathbf{x}|\mathbf{d})$ itself by a histogram, where each sample is counted according to its importance. The highest importance samples then correspond to halos that most resemble that of the MW, in terms of its bright satellite properties.

To calculate the likelihood from N independent data points, we compute the product

$$\Pr(\mathbf{d}|\mathbf{x}) = \prod_i^N \frac{1}{\sqrt{2\pi}\sigma_i} \exp\left[-\frac{(d_i - d_i^p(\mathbf{x}))^2}{2\sigma_i^2}\right], \quad (3)$$

where we take the individual likelihood functions to have Gaussian form. The predicted data $d_i^p(\mathbf{x})$ are quantities that we can compute from the halo parameters \mathbf{x} and are compared to our measured data via this likelihood. We use the data values $d_i = \{v_{\max}, r_0, v_r, s\}_i$ and their uncertainties σ_i , as given in Table 1.

There are three additional steps in our inference we must note. First, because of the very tight constraints on the positions of the MCs, we choose not to weight them by the error in their measurement, but by 5 times the error, effectively requiring that our simulated analogs be within 10 kpc of the observed MC locations. Second, because of the very tight observational constraints on the properties of the MCs, relatively few Bolshoi halos receive significant importance. We compensate for this by stacking multiple simulation outputs to improve the statistics of our sample, rejecting any repeat appearances of the same halo. Finally, the lack of treatment of baryons in Bolshoi introduces a systematic error. Because the more concentrated mass in the stellar disk at the halo center should increase the speed of the satellites orbiting their hosts at small radii, we increase the total velocity of all satellites by the circular velocity due to the stellar disk, $v_{\text{circ}} = \sqrt{GM_*/r_{\text{sat}}}$, where $M_* = 6 \times 10^{10} M_{\odot}$ (Klypin et al. 2002). By performing our analysis twice, with and without this velocity correction, we can get an approximate upper limit on the size of the systematic error due to baryon physics.

5. THE MASS DISTRIBUTION OF THE MILKY WAY

Figure 1 (left panel) shows the posterior PDF for the MW halo mass, computed by weighting every Bolshoi halo by the probability that its bright satellite population looks like that of the MW in various ways. Some observations provide significantly more information about the host halo mass than others: the distance to and radial velocity of the MCs are most constraining, while the maximum circular velocity of the LMC and SMC provide almost no information (largely due to their measurement errors). Note that it is the *combination* of datasets that is most important, as internal degeneracies are broken, i.e., there is a high degree of covariance between positional and kinematic properties. The combination of all datasets gives $M_{\text{MW}} = 1.2^{+0.7}_{-0.4} \times 10^{12} M_{\odot}$ (68% confidence) and a virial radius $r_{\text{vir}} = 250^{+60}_{-30} \text{ kpc}$. Repeating this without the baryon correction increases the typical masses, and implies a maximum systematic error of $\log(M_{\text{MW}}) = 0.2$. While many more halos contribute statistically to the inference, we find 22 1σ matches (systems that are an average of 1σ away from observations of the MCs in the 8 properties listed in Table 1) and more than 200 2σ matches in the 60 snapshots.

Figure 1 (right panel) compares our result with previous MW halo mass estimates from the literature. The LMC and SMC properties lead to a halo mass that is in excellent agreement with the dynamical estimates in the literature. In particular, our results are in near perfect agreement with the most recent stellar velocity measurements (Xue et al. 2008), with similar error bars.

Throughout the paper, we refer to collection of hosts weighted by the v_{\max} , r_0 , v_r , and s of their satellites as “satellite analogs” of the MW. Note that this does not imply that we have selected a specific subset of hosts. Rather, we have taken *all* hosts with $N_{\text{subs}} = 2$ and weighted each object by its satellite properties. It is this sample of weighted objects that defines our satellite analogs. It is worth noting, however, while we formally use all 35,000 $N_{\text{subs}} = 2$ halos in Bolshoi, the ~ 200 1- and 2- σ halos provide more than 95% of the total

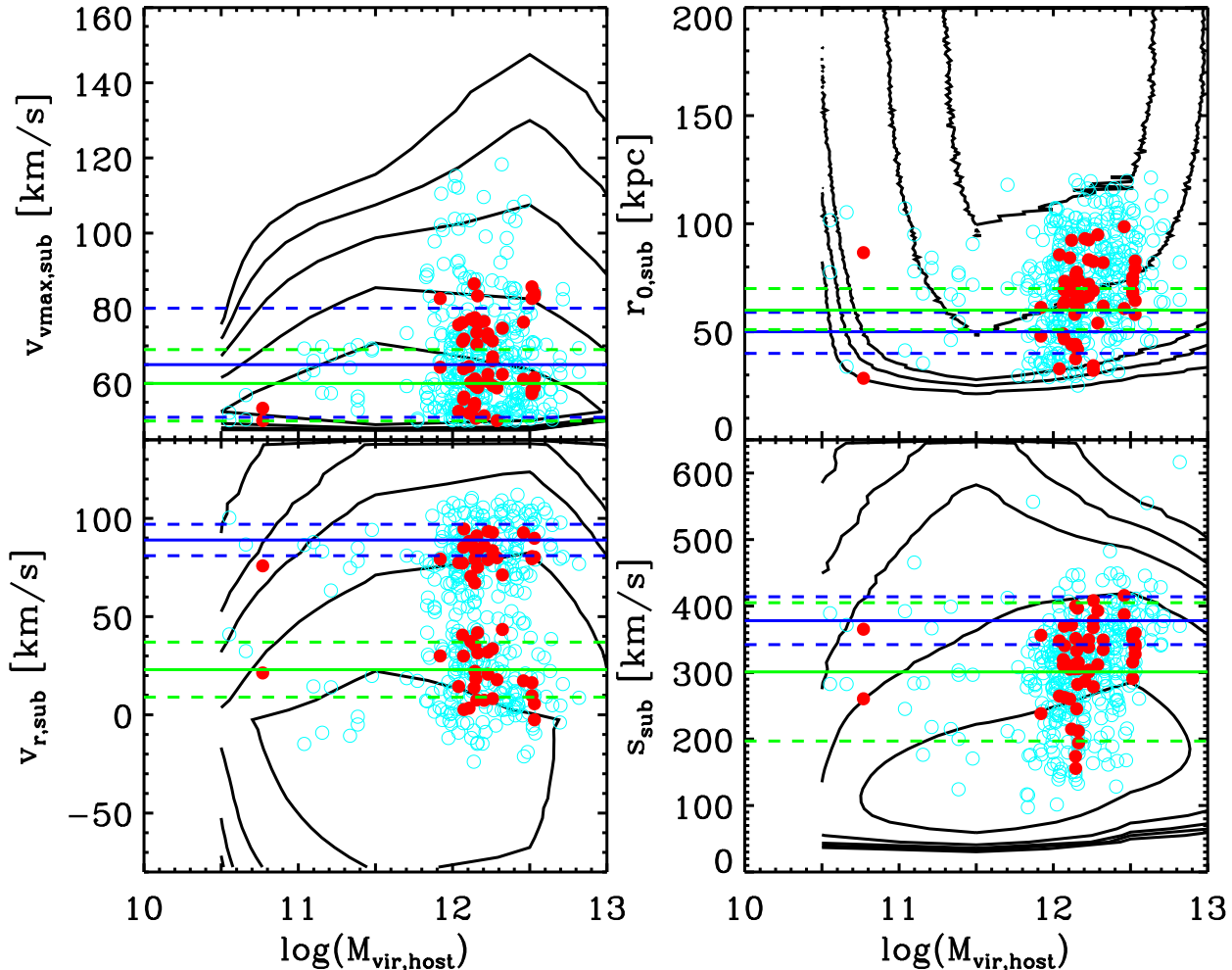


FIG. 2.— Covariance between $M_{\text{vir,host}}$ and various satellite properties: v_{max} (top left), r_0 (top right), v_r (bottom left), and s (bottom right). In all panels, the black contours show the regions containing 68, 90, 95, 98, and 99% of our prior distribution, all satellites in a host with $N_{\text{sub}} = 2$. The open cyan and filled red circles denote the satellites for 2- and 1- σ halos. Blue and green lines show the observed values and $\pm 1-\sigma$ uncertainty for each property, for the LMC and SMC respectively.

weight.

Because we want to further understand what impact the MCs have on other halo properties, we also define “mass analogs” to be set of halos randomly drawn from the mass PDF of the satellite analogs. Thus, the mass analogs have the same PDF of virial masses as the black line of Figure 1, but no constraints on their satellite properties. Comparison between our satellite analogs and mass analogs allows us to disentangle impacts on the system due to the satellite properties from those due to the particular mass range probed by our satellite analogs.

When interpreting Figure 1, it is also helpful to consider the full dependence of the predicted satellite properties on the mass of the host halos. This is shown in Figure 2, which compares the trends of v_{max} , r_0 , v_r , and s for the satellites with the M_{vir} of their hosts. The plots show contours containing 68, 90, 95, 98, and 99% of our prior probability (that is, all hosts with exactly two satellites, black lines), as well as the exact locations of our 2- σ (open cyan circles) and 1- σ hosts (filled red circles). Also plotted are the observed properties of the LMC

and SMC (blue and green lines). These plots highlight a number of important trends. First, we can see that the MCs are atypical subhalos in most regards. The LMC in particular is roughly a 2- σ outlier in each of these properties. Second, covariances can be seen, such as the degeneracy between speed and host mass, which shows explicitly how the high speed of the satellites pushes the likelihood towards higher mass hosts. Additionally, it is interesting to note that, while rare, there are a handful of objects with $M_{\text{vir}} < 10^{11} M_{\odot}$ with satellites that are well matched to the MCs. The satellites of these low-mass halos are not energetically bound to their hosts. Finally, while it can be seen that observations of s provide the most stringent constraints individually, these plots further emphasize that it is the combination of observed properties that is necessary to place tight constraints on M_{MW} .

We can also determine the impact of the MCs on the internal mass distribution of a halo by comparing the density profiles for our satellite and mass analogs. This gives us a handle on how typical the MW is for a halo of its mass. We find that the presence of the MCs has only a modest impact on

the halo concentration, but can impact density profiles significantly in other ways. In particular, when looking at the mass enclosed within a fixed 8 kpc (the distance from the sun to the center of the galaxy), satellite analogs have a 60% higher central density than mass analogs. This tells us that the MCs are correlated with a more strongly peaked inner dark matter distribution. For the full density profile (which includes contributions from substructures), however, satellite analogs have $c = 11 \pm 2$, a little less than $1\text{-}\sigma$ higher than $c = 8.7 \pm 3.5$ for the mass analogs. While this still implies a correlation between the presence of the MCs and a more peaked mass distribution, it shows that the impact is much weaker at larger radii than it is for the central core.

6. THE ASSEMBLY OF THE MILKY WAY HALO

We now turn our attention to the assembly history of the Milky Way. We use the same importance-sampled halos from the previous section to infer the MW assembly history, in the same way as we inferred its mass and density profile. Figure 3 shows the distribution of accretion times for these satellite analogs; we also show the accretion time PDF for all hosts with $N_{\text{subs}} = 2$, and for the mass analog systems defined above. The mass analogs (red line) clearly show two populations. The first consists of halos whose subhalos were accreted at high redshift, when the host halo was in its exponential growth phase, which suppresses tidal stripping of the subhalos (Wechsler et al. 2002; Busha et al. 2007). The second population consists of halos with recently accreted objects that have not had enough time to undergo significant tidal disruption. The relative size of these populations changes when we apply the observational likelihoods. Requiring that a host has $N_{\text{subs}} = 2$ massive subhalos (with unconstrained speeds and distances, dotted line) has little impact. However, for satellite analogs (black line), the size of the recently accreted population increases dramatically. This is primarily driven by the combined requirement that the satellites have both a high radial velocity and are close to the center of the halo, and argues that there is roughly a 72% chance that MCs are recent arrivals, accreted within the past 1 Gyr.

Did the MCs arrive together? Figure 4 shows the difference in accretion times, Δt_{acc} , for the two most massive satellites of all hosts with $N_{\text{subs}} = 2$ and for the two satellites of the satellite analog hosts. For satellite analogs, the distribution is strongly peaked towards small Δt_{acc} , with roughly 50% of satellites having been accreted simultaneously (within a Gyr of each other). These simultaneous accretions correspond very tightly with the recently accreted population. The noise in this plot, and in particular the peak around $\Delta t_{\text{acc}} \approx 8\text{--}9$ is driven by a few very well matched (high weight) halos that had one one satellite accrete within the last Gyr and the other early on during the exponential buildup phase (see the weaker secondary peak in Figure 3). This highlights the current level of noise in our analysis due to our modest statistical size. We anticipate that, with better statistics, this high- Δt_{acc} bump will smooth out, making a smoother distribution that is even more sharply peaked at $\Delta t_{\text{acc}} = 0$. For comparison, halos with $N_{\text{subs}} = 2$, shown as the dashed line, have a much weaker preference for simultaneous accretion.

Both this result and that of Figure 3 favor a method for the creation of the Magellanic Stream other than tidal disruption by the MW, such as such as the model of Besla et al. (2010), who found good agreement with the dynamics the Stream for a model in which it was created by tidal disruption of the SMC by the LMC before they were accreted as a bound

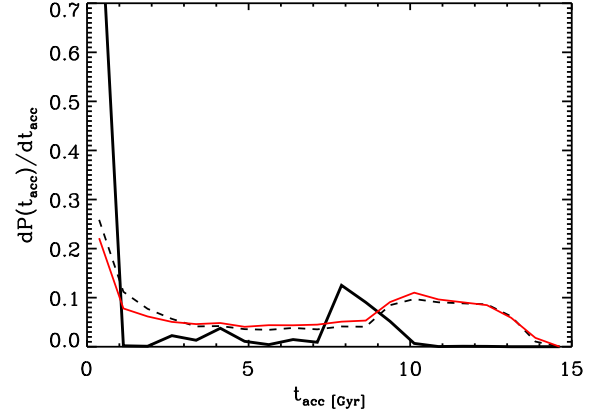


FIG. 3.— Posterior distribution of satellite accretion times, from the MW satellite analogs (black), from hosts with exactly two subhalos (dashed), and from MW mass analogs (red). Selecting hosts with MC-like satellites strongly weights the distribution towards recent accretion.

pair. Additionally, the satellites in the satellite-analogs have a high degree of spatial correlation, with a typical separation of 48 ± 8 kpc, about 3σ larger than the observed MC separation of 25 kpc (Kallivayalil et al. 2006a). They are substantially closer to each other than typical systems with $N = 2$, which have separations of ~ 200 kpc.

7. CONCLUSIONS

The advent of high-resolution cosmological simulations which sample the dynamical histories of large numbers of dark matter halos in a wide range of environments provides us with a new approach for determining the properties of individual halos given their observational characteristics. Here, we use the observed properties of the Magellanic Clouds to constrain the mass distribution and assembly history of the Milky Way. In comparison to previous efforts which use detailed observations but a necessarily simplified dynamical model, our approach uses simple observations and statistical inference from sampling of a detailed and cosmologically consistent dynamical model.

Our principal conclusions are:

1. We infer the MW halo mass to be $M_{\text{MW}} = 1.2^{+0.7}_{-0.4} \times 10^{12} M_{\odot}$ (68% confidence), in very good agreement with the recent stellar velocity measurements (Xue et al. 2008), with similarly sized error bars.
2. The MW halo has a slightly higher concentration than is typical for its mass: 11 ± 2 , compared to 8.7 ± 3.5 . Additionally, the density within 8 kpc is 60% higher for satellite analogs than for mass analogs.
3. Typical bright satellites of halos with MW mass were accreted at a range of epochs, generally at high redshift (c. 10 Gyr ago) or much more recently (within the last 2 Gyr). Because of their high speed near the center of the halo, we find a 72% probability that the Magellanic Clouds were accreted within the last Gyr. We also find a 50% probability that the MCs were accreted within 1 Gyr of each other.

This approach clearly allows one to explore a wide range of additional properties of MW-like halos; however, it places challenging requirements on the simulations used. In particular, for MW studies we are still limited by the relatively small

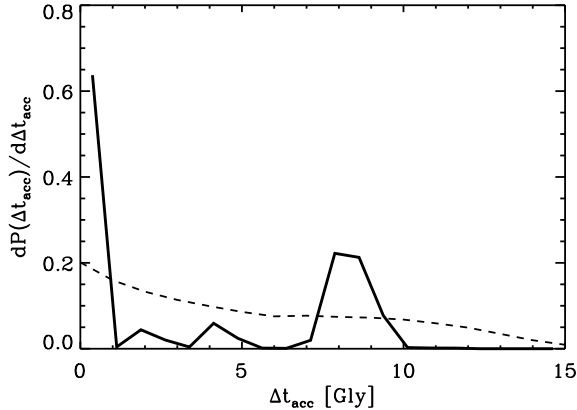


FIG. 4.— Difference between accretion times for the two most massive satellites in MW-like systems. The solid line represents satellite analogs; dashed line shows all systems with exactly two subhalos.

simulation volume used. With the constraints used here, we found just one good fit halo per $\sim 500\text{Mpc}^3$, emphasizing the large volume required to perform this analysis. As more criteria are applied we will need to sample a larger range of formation histories and environments drawn from a larger cosmological volume. In addition, the properties of its smaller satellites are not accessible with our present resolution. Pushing forward on both simulated resolution and volume will be essential to realize the full potential of this approach. Additionally, the simulations used here ignore the impact of baryons on the dark matter distribution. We have included a simple model of the stellar disk which is applied to the satellite velocities to get a handle on the impact of this systematic, but the model is

simplistic and the effects of the baryonic component need to be further studied.

As we were completing this work, Boylan-Kolchin et al. (2010) presented results from a similar study. Their principal results regarding the mass of the MW and the accretion history of the LMC and SMC are in reasonable agreement with our own, although they favor a somewhat larger MW mass. The primary difference between these works is the larger volume simulation used here, as well as our use of statistical inference. Additionally, significantly different selection criteria for identifying “MW-like” objects were employed. Boylan-Kolchin et al. (2010) selected hosts whose two largest subhalos were within $0.75 r_{200}$ and had similar stellar masses to the MCs using abundance matching to estimate the stellar content of their simulated halos. In this work, we select objects with exactly two subhalos more massive than $v_{\text{max}} = 50\text{km s}^{-1}$ within a fixed 300 kpc aperture and then weight our sample according to how well the subhalos look like the MCs in terms of v_{max} , position, radial velocity, and total speed. These differences likely account for the tension in the resulting M_{MW} PDFs.

MTB and RHW were supported by the National Science Foundation under grant NSF AST-0807312. PJM acknowledges the Kavli Foundation and the Royal Society for support in the form of research fellowships. We thank Louie Strigari, Brian Gerke, Nitya Kallivayalil, and Gurtina Besla for useful discussions. The Bolshoi simulation was run using NASA Advanced Supercomputing resources at NASA Ames Research Center.

REFERENCES

- Battaglia, G., et al. 2005, *MNRAS*, 364, 433
 Belokurov, V., et al. 2007, *ApJ*, 654, 897
 Besla, G., Kallivayalil, N., Hernquist, L., Robertson, B., Cox, T. J., van der Marel, R. P., & Alcock, C. 2007, *ApJ*, 668, 949
 Besla, G., Kallivayalil, N., Hernquist, L., van der Marel, R. P., Cox, T. J., & Kereš, D. 2010, *ApJ*, 721, L97
 Boylan-Kolchin, M., Besla, G., & Hernquist, L. 2010, *ArXiv e-prints*
 Busha, M. T., Evrard, A. E., & Adams, F. C. 2007, *ApJ*, 665, 1
 Busha, M. T., Wechsler, R. H., & Behroozi, P. 2010, *ApJ*, to be submitted
 Connors, T. W., Kawata, D., & Gibson, B. K. 2006, *MNRAS*, 371, 108
 Conroy, C., Wechsler, R. H., & Kravtsov, A. V. 2006, *ApJ*, 647, 201
 Dehnen, W., McLaughlin, D. E., & Sachania, J. 2006, *MNRAS*, 369, 1688
 D’Onghia, E., & Lake, G. 2008, *ApJ*, 686, L61
 Gardiner, L. T., Sawa, T., & Fujimoto, M. 1994, *MNRAS*, 266, 567
 Gnedin, O. Y., Brown, W. R., Geller, M. J., & Kenyon, S. J. 2010, *ApJ*, 720, L108
 Harris, J., & Zaritsky, D. 2006, *AJ*, 131, 2514
 Kallivayalil, N., van der Marel, R. P., & Alcock, C. 2006a, *ApJ*, 652, 1213
 —, 2006b, *ApJ*, 652, 1213
 Kallivayalil, N., van der Marel, R. P., Alcock, C., Axelrod, T., Cook, K. H., Drake, A. J., & Geha, M. 2006c, *ApJ*, 638, 772
 Klypin, A., & Holtzman, J. 1997, *ArXiv Astrophysics e-prints*
 Klypin, A., Trujillo-Gomez, S., & Primack, J. 2010, *ArXiv e-prints*
 Klypin, A., Zhao, H., & Somerville, R. S. 2002, *ApJ*, 573, 597
 Kravtsov, A. V., Berlind, A. A., Wechsler, R. H., Klypin, A. A., Gottlöber, S., Allgood, B., & Primack, J. R. 2004, *ApJ*, 609, 35
 Kravtsov, A. V., Klypin, A. A., & Khokhlov, A. M. 1997, *ApJS*, 111, 73
 Kuhlen, M., Weiner, N., Diemand, J., Madau, P., Moore, B., Potter, D., Stadel, J., & Zemp, M. 2010, *JCAP*, 2, 30
 Lewis, A., & Bridle, S. 2002, *Phys. Rev. D*, 66, 103511
 Li, Y., & White, S. D. M. 2008, *MNRAS*, 384, 1459
 Lisanti, M., Strigari, L. E., Wacker, J. G., & Wechsler, R. H. 2010, *ArXiv e-prints*
 Liu, L., Gerke, B., Wechsler, R., Behroozi, P., & Busha, M. 2010, *ApJ*, to be submitted
 Murai, T., & Fujimoto, M. 1980, *PASJ*, 32, 581
 Piatek, S., Pryor, C., & Olszewski, E. W. 2008, *AJ*, 135, 1024
 Smith, M. C., et al. 2007, *MNRAS*, 379, 755
 Stanimirović, S., Staveley-Smith, L., & Jones, P. A. 2004, *ApJ*, 604, 176
 Strigari, L. E., Bullock, J. S., Kaplinghat, M., Diemand, J., Kuhlen, M., & Madau, P. 2007, *ApJ*, 669, 676
 Strigari, L. E., & Trotta, R. 2009, *Journal of Cosmology and Particle Physics*, 11, 19
 Suyu, S. H., Marshall, P. J., Auger, M. W., Hilbert, S., Blandford, R. D., Koopmans, L. V. E., Fasnacht, C. D., & Treu, T. 2010, *ApJ*, 711, 201
 Tollerud, E. J., Bullock, J. S., Strigari, L. E., & Willman, B. 2008, *ApJ*, 688, 277
 van den Bergh, S. 2000, *The Galaxies of the Local Group*, ed. van den Bergh, S. (Cambridge)
 van der Marel, R. P., Alves, D. R., Hardy, E., & Suntzeff, N. B. 2002, *AJ*, 124, 2639
 Vogelsberger, M., et al. 2009, *MNRAS*, 395, 797
 Walsh, S. M., Willman, B., & Jerjen, H. 2009, *AJ*, 137, 450
 Watkins, L. L., Evans, N. W., & An, J. H. 2010, *MNRAS*, 406, 264
 Wechsler, R. H., Bullock, J. S., Primack, J. R., Kravtsov, A. V., & Dekel, A. 2002, *ApJ*, 568, 52
 Xue, X. X., et al. 2008, *ApJ*, 684, 1143